discharged on POD 100 without abnormal fluid collection around the pancreas (fig 9). The patient is well and receiving a regular out-patient treatment showing no recurrence of pancreatic fistula.

DISCUSSION

Pancreatic fistula is primarily treated by conservative therapy, which includes rapid total infusion or enteral nutrition along with administration of octreotide. The recovery rate after conservative therapy ranges from 44% to 85%[6-8]; thus, a number of cases are not resolved by conservative treatment. Surgical treatment has been performed in such cases. However, surgical treatment is highly invasive and may lead to various complications. Further, surgical treatment is associated with high mortality rates, with the mortality rate being as high as 23%-67% in the cases showing early peritonitis after the operation[9]. Endoscopic drainage of the main pancreatic duct via the ampulla of Vater, which was first reported in 1991[10], has drawn considerable attention. Boerma et al. (2006) reported an excellent recovery rate (87%) after endoscopic treatment of 15 cases of pancreatic fistula[11]. In addition, other studies have reported recovery rates of about 58%-100% in the cases of pancreatic fistulas that do not

respond to conservative therapy and involve endoscopic treatment[12-20]. To date, only 1 death caused by acute pancreatitis has been reported. However, since this death may also have been caused by inadequate drainage, a direct relationship between the death and endoscopic treatment could not be confirmed[13]. Unlike LDLT, endoscopic treatment for pancreatic fistula allows greater accessibility to the ampulla of Vater. Further, endoscopic treatment is less invasive than surgical treatment; therefore, it can easily replace conservative therapy if sufficient drainage is achieved. Thus, patients who undergo endoscopic treatment for pancreatic fistula can be expected to make an early recovery. Irrespective of their merits and demerits, both ENPD and endoscopic pancreatic stenting (EPS) have been referred to in the reports. ENPD causes a sense of discomfort in the pharynx; however, this technique enables easy diagnosis of occlusion and dropout because it allows monitoring of the pancreatic fluid. In contrast, in EPS, the diagnosis of occlusion and dropout is difficult; however, this technique causes no sense of discomfort in the pharynx. We selected ENPD to enable safe monitoring of 2 channels of drainage: the endoscopic retrograde pancreatic drain as well as the interperitoneal drain. In case 1, the drain tube had to be replaced because of the fever caused by

occlusion; therefore, the choice of ENPD was considered to be reasonable. The patient in case 1 could have recovered earlier if the endoscopic treatment for pancreatic fistula had been initiated earlier. In each case, the patient recovered within approximately 40 days after ENPD. Further, the treatment had no influence on the patients' general status. Endoscopic treatment is considered to be safe for treating pancreatic fistulas that develop after LDLT. New endoscopic techniques, such as ultrasonography (US)-guided drainage, have also been used to treat refractory cases that do not respond to drainage via the ampulla of Vater; however, only few reports have described these techniques. These new techniques may also be less invasive than surgical treatment[21-22].

In conclusion, we described 2 cases of pancreatic fistula after LDLT that were not responsive to conservative therapy. In each case, the patient recovered within approximately 40 days after ENPD. Thus, endoscopic treatment for pancreatic fistula after LDLT should be adopted because of its high recovery rate and low invasiveness.

REFERENCES

1. Freise CE, Gillespie BW, Koffron AJ et al. Recipient morbidity after living and deceased donor liver transplantation: findings from the A2ALL Retrospective Cohort Study. Am J Transplant 2008; 8:2569-2579. PMID: 18976306

2. Ho MC, Wu YM, Hu RH et al. Surgical complications and outcome of living related liver transplantation. Transplant Proc 2004; 36:2249-2251. PMID: 15561208

3. Marsh JW, Gray E, Ness R et al. Complications of right lobe living donor liver transplantation. J Hepatol 51:715-724. 2009;_PMID: 19576652

4. Emiroglu R, Sevmis S, Moray G et al. Living-donor liver transplantation: results of a single center. Transplant Proc 2007; 39:1149-1152. PMID: 17524917

5. Tanaka K, Miyashiro I, Yano M et al. Accumulation of excess visceral fat is a risk factor for pancreatic fistula formation after total gastrectomy. Ann Surg Oncol 2009; 16:1520-1525._PMID: 19267237

6. Parr ZE, Sutherland FR, Bathe OF et al. Pancreatic fistulae: are we making progress? J Hepatobiliary Pancreat Surg 2008; 15:563-569.

7. Pratt WB, Maithel SK, Vanounou T et al. Clinical and economic validation of the International Study Group of Pancreatic Fistula (ISGPF) classification scheme. Ann Surg 2007; 245:443-451. PMID: 18987924

8. Lipsett PA, Cameron JL. Internal pancreatic fistula. Am J Surg 1992; 163:216-220. PMID: 1739176

9. Tung BY, Kowdley KV, Kimmey MB. Pancreatic fistula without pancreatitis after endoscopic biliary stent placement for bile leak after orthotopic liver transplantation. Gastrointest Endosc 1999; 49:647-651. PMID: 10228269

10. Kozarek RA, Ball TJ, Patterson DJ et al. Endoscopic transpapillary therapy for disrupted pancreatic duct and peripancreatic fluid collections. Gastroenterology 1991; 100:1362-1370. PMID: 2013381

11. Boerma D, Rauws EA, van Gulik TM et al. Endoscopic stent placement for pancreaticocutaneous fistula after surgical drainage of the pancreas. Br J Surg 2000; 87:1506-1509.

12. Bracher GA, Manocha AP, DeBanto JR et al. Endoscopic pancreatic duct stenting to treat pancreatic ascites. Gastrointest Endosc 1999; 49:710-715. PMID: 11091237

13. Telford JJ, Farrell JJ, Saltzman JR et al. Pancreatic stent placement for duct disruption. Gastrointest Endosc 2002; 56:18-24. PMID: 12085030

14. Varadarajulu S, Noone TC, Tutuian R et al. Predictors of outcome in pancreatic duct disruption managed by endoscopic transpapillary stent placement. Gastrointest Endosc 2005; 61:568-575. PMID: 15812410

15. Saeed ZA, Ramirez FC, Hepps KS. Endoscopic stent placement for internal and external pancreatic fistulas. Gastroenterology 1993; 105:1213-1217. PMID: 8405869

16. Kozarek RA, Ball TJ, Patterson DJ et al. Transpapillary stenting for pancreaticocutaneous fistulas. J Gastrointest Surg 1997; 1:357-361. PMID: 9834370

17. Costamagna G, Mutignani M, Ingrosso M et al. Endoscopic treatment of postsurgical external pancreatic fistulas. Endoscopy 2001; 33:317-322. PMID: 11315892

18. Fischer A, Benz S, Baier P et al. Endoscopic management of pancreatic fistulas secondary to intraabdominal operation. Surg Endosc 2004; 18:706-708. PMID: 15026901

19. Le Moine O, Matos C, Closset J et al. Endoscopic management of

pancreatic fistula after pancreatic and other abdominal surgery. Best Pract Res Clin Gastroenterol 2004; 18:957-975. PMID: 15494289

20. Goasguen N, Bourrier A, Ponsot P et al. Endoscopic management of pancreatic fistula after distal pancreatectomy and enucleation. Am J Surg 2009; 197:715-720. PMID: 18789426

21. Romano A, Spaggiari M, Masetti M et al. A new endoscopic treatment for pancreatic fistula after distal pancreatectomy: case report and review of the literature. Gastrointest Endosc 2008; 68:798-801. PMID: 18514650

22. Arvanitakis M, Delhaye M, Bali MA et al. Endoscopic treatment of external pancreatic fistulas: when draining the main pancreatic duct is not enough. Am J Gastroenterol 2007; 102:516-524. PMID: 17335445

S editor Tian L L editor E editor

Figure Legend

Fig 1: Computed tomography (CT) performed on postoperative day (POD) 13 showing fluid collection (circle) at the lower edge of the pancreas. The hematoma was considered to be ruptured.

Fig 2: Pancreatographic examination of the drain at the tail of the pancreas (Drain) in case 1 reveals the disrupted (arrows) main pancreatic duct (MPD) with flow of contrast into the duodenum.

Fig 3: A radiograph showing postprocedure endoscopic naso-pancreatic drainage (ENPD) in case 1. Excellent drainage of the pancreatic duct is noted.

Fig 4: Upper chart shows the body temperature (BT) and serum C-reactive protein (CRP) level. Lower one shows daily output of the endoscopic naso-pancreatic drainage (ENPD) tube and the drain at the tail of the pancreas (Tail) in case 1. The patient had an episode of fever caused by the occlusion of the ENPD tube. After the tube was replaced, the pancreatic fistula healed completely.

Fig 5: Contrast examination from the drain at the tail of the pancreas (Drain) in case 1 on postoperative day (POD) 363 reveals the closure of fistula.

Fig 6: Computed tomography (CT) performed 2 days after removal of the drain in case 1 showing no fluid collection around the pancreas.

Fig 7: A radiograph showing postprocedure endoscopic naso-pancreatic drainage (ENPD) in case 2. The image shows drains placed at both the right and left edges of the pancreas (Right and Left) and ENPD.

Fig 8: Upper chart shows the body temperature (BT) and serum C-reactive protein (CRP) level. Lower one shows daily output of endoscopic naso-pancreatic drainage (ENPD) tube and the drains at both the edges of the pancreas (Right and Left) in case 2. The pancreatic fistula healed completely on post-ENPD day 38.

Fig 9: Computed tomography (CT) performed 14 days after removal of the drains in case 2 showing no fluid collection around the pancreas.

LIVER TRANSPLANTATION 16:1062-1068, 2010

ORIGINAL ARTICLE

Three-Dimensional Computed Tomography Scan Analysis of Hepatic Vasculatures in the Donor Liver for Living Donor Liver Transplantation

Koichiro Uchida,[1] Masahiko Taniguchi,[2] Tsuyoshi Shimamura,[3] Tomomi Suzuki,[2] Kenichiro Yamashita,[4] Minoru Ota,[3] Toshiya Kamiyama,[1] Michiaki Matsushita,[1] Hiroyuki Furukawa,[2] and Satoru Todo[1]

[1]Department of General Surgery, [2]Department of Organ Transplantation and Regeneration, [3]Division of Organ Transplantation, and [4]Department of Molecular Surgery, Graduate School of Medicine, Hokkaido University, Sapporo, Japan

Because hepatic vasculatures exhibit variations, a preoperative evaluation of the vascular anatomy and an estimation of the volume of the liver graft are essential for successful adult living donor liver transplantation. Using 3-dimensional (3D) computed tomography (CT), we analyzed the volumetric and anatomical relationship of the hepatic vasculatures of liver grafts. The livers of 223 potential donors were analyzed by 3D CT. Volumetric analysis was performed for each hepatic vein and its tributaries. The anatomy of the portal vein and hepatic artery was assessed along with the biliary system via intraoperative cholangiography in 110 recipients. On the basis of the anatomical presentation of the inferior right hepatic vein (IRHV), the hepatic veins were classified as follows: in type I, the IRHV was absent; in type II, the IRHV was smaller than the right hepatic vein (RHV); and in type III, the IRHV was greater than or equal to the RHV in size. The drainage volume of the middle hepatic vein (MHV) and especially its tributaries in the right lobe increased with the size of the IRHV ($P < 0.001$). In type III hepatic veins with a large IRHV (17% of the donors), the MHV tributaries had the largest drainage volume in the right lobe (41.2% ± 11.8%). Furthermore, type III hepatic veins typically exhibited biliary variations in 75% of the donors. No correlation was observed between variations in the hepatic artery and portal vein. In conclusion, a right lobe graft with a large IRHV is accompanied by a large drainage volume via the MHV and by bile duct variations in 17% of livers. Therefore, anatomical and volumetric analysis is important for preoperative evaluations. ***Liver Transpl 16:1062-1068, 2010.*** © **2010 AASLD.**

Received January 16, 2010; accepted May 17, 2010.

Living donor liver transplantation (LDLT) is an alternative to deceased donor liver transplantation for the treatment of patients with end-stage liver disease.[1] However, its application in adult recipients has been complicated by the problems associated with anatomical variations of hepatic vasculatures[2] and insufficient graft volume caused by venous outflow disturbances.[3] This is particularly true when the right lobe is selected for transplantation.

To successfully perform right lobe LDLT, the drainage volume of the middle hepatic vein (MHV) tributaries and the inferior right hepatic vein (IRHV) must be

Abbreviations: 3D, 3-dimensional; A1, normal branching of the hepatic artery; A2, replacement of the left hepatic artery from the left gastric artery; A3, replacement of the right hepatic artery from the superior mesenteric artery; A4, middle hepatic artery arising from the left hepatic artery; A5, middle hepatic artery arising from the right hepatic artery; B1, normal branching of the biliary duct; B2, trifurcation of the biliary duct; B3, posterior branching from the left hepatic duct; B4, independent posterior branching from the common hepatic duct; B5, segment 3 or 4 bile duct from the right hepatic duct; CT, computed tomography; IRHV, inferior right hepatic vein; LDLT, living donor liver transplantation; LGA, left gastric artery; LHV, left hepatic vein; MHA, middle hepatic artery; MHV, middle hepatic vein; NS, not significant; PHA, proper hepatic artery; PV1, normal branching of the portal vein; PV2, trifurcation of the portal vein; PV3, independent branching of the posterior branch from the main portal trunk; RHV, right hepatic vein; SMA, superior mesenteric artery; V5, vein draining segment 5; V8, vein draining segment 8.

Address reprint requests to Masahiko Taniguchi, M.D., Department of Organ Transplantation and Regeneration, Graduate School of Medicine, Hokkaido University, N-15, W-7, Kita-Ku, Sapporo 060-8638, Japan. Telephone: +81-11-706-7062; FAX: +81-11-706-7064; E-mail: m-tani@med.hokudai.ac.jp

DOI 10.1002/lt.22109
View this article online at wileyonlinelibrary.com.
LIVER TRANSPLANTATION.DOI 10.1002/lt. *Published on behalf of the American Association for the Study of Liver Diseases*

considered.[4] Liver atrophy or almost no liver regeneration has been noted in congested areas.[5] Moreover, large congested areas can also result in infarction and lead to septic shock.[3] Complications caused by potentially congested areas can be prevented if an adequate volume is provided by venous reconstruction, even in a right lobe graft with large congested areas.[6] Meanwhile, extended right lobe grafts[7] or right lobe grafts in which venous collaterals are preserved without reconstruction of MHV branches[8] have been used to manage graft congestion and to provide consistent graft function. However, an extended right lobe graft leads to congestion of the left medial segment in the donor. Because of these findings, a right lobe graft with reconstruction of the MHV is still more common.

In the right lobe graft, multiple branches of the portal vein (8.1%-13.6%),[9-11] hepatic artery (18%),[12] and bile duct (41.5%-67.5%)[13] can be exposed on the cut surface. In such cases, multiple or complex reconstructions are necessary, and this may increase the attendant risk of anastomotic complications.[12,14-16]

In recent years, 3-dimensional (3D) computed tomography (CT) scans have assisted doctors in preoperative surgical planning. We have reported the contribution of 3D CT scans in evaluating the morphology of hepatic vessels and tumors and in estimating the volume that is drained from the liver by the hepatic vein.[17-19] Previously, the morphology of each hepatic vein pattern has been classified individually as surgical anatomy for hepatectomy. Reichert et al.[20] classified the left hepatic vein (LHV), Marcos et al.[4] and Neumann et al.[21] classified the MHV, and Radtke et al.[22] classified the IRHV. Nakamura and Tsuzuki[23] reported the size of the right hepatic vein (RHV) in a case study. The RHV is generally the largest draining vein in both the right lobe and the whole liver, although the size of the RHV varies according to the size of the IRHV.[23] The morphology or interrelationship of each hepatic vein (especially the RHV and MHV) is important for successful reconstruction in LDLT.

In the current study, we attempted to analyze the volumetric and anatomical interrelationships of the hepatic veins (RHV, MHV, and IRHV) and other hepatic vasculatures (portal vein, hepatic artery, and bile duct) in LDLT. Our results indicate that a knowledge of these associations contributes to preoperative evaluations of the donor liver in LDLT.

PATIENTS AND METHODS

Patients

From August 2002 to May 2009, 223 potential liver donors were analyzed with 3D analysis software at Hokkaido University Hospital (Sapporo, Japan). One hundred thirteen were donor candidates, and 110 subsequently underwent surgery as donors for graft harvesting. None of the analyzed potential donors had a fatty liver on the CT scan.

CT Scan and Volume Rendering

All CT scans were obtained with a 64-slice multidetector CT scanner (Aquilion, Toshiba, Tokyo, Japan). All data were transferred to a 3D workstation (Virtual Place Lexus, Medical Imaging Laboratory, AZE, Tokyo, Japan). A virtual dissection line was drawn between the left and right lobes of the liver (determined from the Rex-Cantlie line) just above the main trunk of the MHV. Both the volume of the whole liver and the right and left lobes and the drainage volume of each hepatic vein and its branches were calculated.

Hepatic Venous Anatomy and Terminology

The names of the hepatic veins and their branches were described according to Couinaud's segmentation[24]; for example, the vein draining segment 5 (the inferior part of the anterior sector) was named V5. Each branch described by 3D CT was more than 2 mm in diameter. The MHV was divided into MHV tributaries in the right lobe and in the left lobe. Assuming right lobe graft LDLT, we analyzed the morphology, drainage volume, and relationships of the hepatic veins (eg, RHV, MHV, and IRHV).

Portal Vein (Fig. 1)

The branching patterns of the portal vein were classified with 3D CT images as follows: normal branching of the portal vein (PV1), trifurcation of the portal vein (PV2), and independent branching of the posterior branch from the main portal trunk (PV3).

Hepatic Artery (Fig. 1)

The branching patterns of the hepatic artery were detected by 3D CT scanning and were denoted as follows: normal branching of the hepatic artery (A1), replacement of the left hepatic artery from the left gastric artery (A2), and replacement of the right hepatic artery from the superior mesenteric artery (A3). The branching patterns of the middle hepatic artery (MHA) were also classified: the MHA arising from the left hepatic artery (A4) and the MHA arising from the right hepatic artery (A5).

Biliary Duct (Fig. 1)

The evaluation of the biliary duct was performed in only 110 donors who underwent intraoperative cholangiography. Branching of the biliary tree was classified as follows: normal branching of the biliary duct (B1), trifurcation of the biliary duct (B2), posterior branching from the left hepatic duct (B3), independent posterior branching from the common hepatic duct (B4), and a segment 3 or 4 bile duct from the right hepatic duct (B5).

Definitions of the Normal and Variation Groups

Considering right and left lobe graft liver transplantation, we classified each branching pattern of the

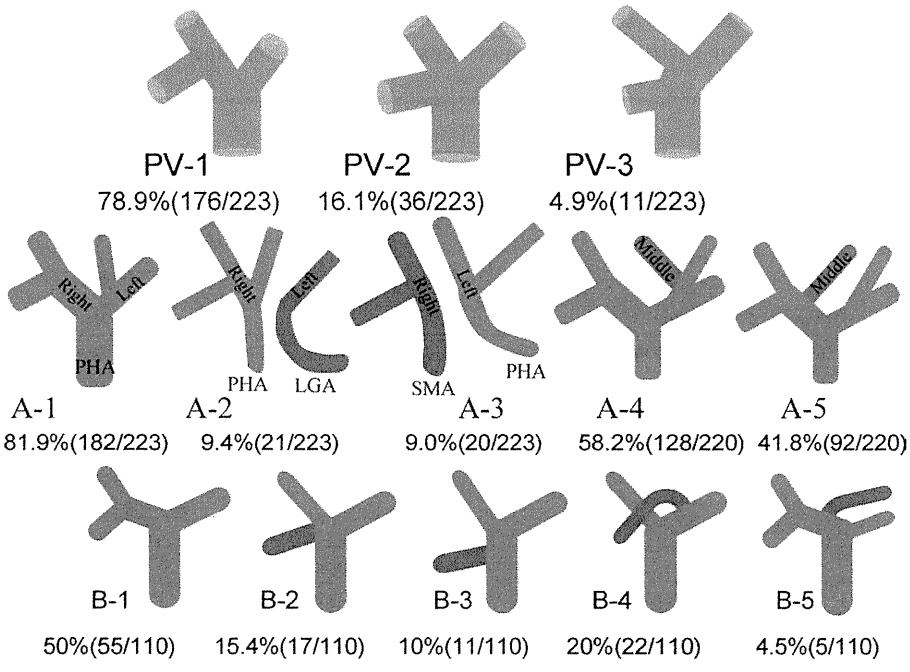

Figure 1. Branching patterns of the portal vein (PV1-PV3), hepatic artery (A1-A5), and biliary duct (B1-B5).

hepatic vasculatures (portal vein and biliary duct) into group A (1 anastomosis in reconstruction) or group B (possible multiple or technically complicated anastomoses). The branching patterns of the hepatic artery were classified into group A (A1 and A3) or group B (A2) for right lobe grafts and into group A (A4) or group B (A5) for left lobe grafts according to the possibility of multiple anastomoses.

Statistical Analysis

Statistical analysis was performed with SPSS version 12.0 (SPSS, Inc., Chicago, IL). Volumetric results are expressed as arithmetic means and standard errors of the mean. Statistical comparisons of the hepatic vasculatures were performed with logistic regression analysis. Volumetric results were compared by 1-way analysis of variance (Tukey). All differences were considered to be statistically significant at $P < 0.05$.

RESULTS

Types of Hepatic Veins

Using 3D CT images, we calculated the drainage volume of each hepatic vein, and we found that the hepatic veins could be classified into 3 types on the basis of the size of the IRHV (Fig. 2). The size of the IRHV was determined by comparison with the RHV. In cases of multiple IRHVs, we evaluated their collective size by determining the drainage volume and comparing it with the RHV volume. The diameter of the IRHV detected by the CT scan in our analysis was >2 mm. The average total volume of the IRHV was 169.5 mL, and the volume ranged from 14 to 556 mL; the average number of IRHVs was 1.24, and the number ranged from 1 to 3.

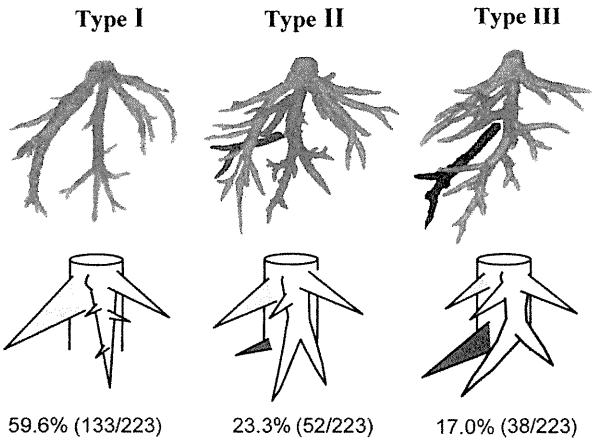

Figure 2. Classification of the hepatic vein by the RHV and IRHV sizes: in type I, the IRHV was absent; in type II, the IRHV was smaller than the RHV; and in type III, the IRHV was greater than or equal to the RHV in size.

Patients with type I hepatic veins had no IRHV, those with type II hepatic veins had a small IRHV (IRHV < RHV), and those with type III hepatic veins had a large IRHV (IRHV ≥ RHV).

Donors and Candidates (Table 1)

In the current study, we investigated the anatomy of the hepatic vasculatures of 113 donor candidates and 110 donors. Comparing the donors and candidates, we found no differences in the type of hepatic vein, the development of each hepatic vein, or the distribution of the branching patterns of the hepatic artery

TABLE 1. Comparison of Donors and Donor Candidates with Respect to the Percentage of Drainage in Whole Liver Grafts by Each Hepatic Vein and with Respect to the Distribution of Branching Patterns of the Hepatic Artery and Portal Vein

Drainage Percentage: Donor Whole Liver				
Vein	Total (n = 110)	Type I (n = 65)	Type II (n = 25)	Type III (n = 20)
RHV	35.6% ± 12.0%	42.4% ± 7.0%	32.2% ± 7.5%	16.3% ± 5.8%*,†,‡
IRHV	5.9% ± 7.2%	0.9% ± 1.5%	8.9% ± 2.9%	18.7% ± 4.1%*,†,‡
MHV	33.7% ± 8.0%	32.1% ± 6.7%	33.2% ± 8.2%	39.6% ± 9.2%†
LHV	20.1% ± 6.4%	20.9% ± 5.2%	19.1% ± 7.9%	18.9% ± 7.7%
Drainage Percentage: Candidate Whole Liver				
Vein	Total (n = 113)	Type I (n = 68)	Type II (n = 27)	Type III (n = 18)
RHV	35.6% ± 12.3%	42.5% ± 7.9%	31.3% ± 8.0%	16.0% ± 5.5%*,†,‡
IRHV	5.85% ± 8.19%	0.7% ± 1.6%	8.6% ± 3.1%	20.8% ± 7.9%*,†,‡
MHV	33.8% ± 8.1%	32.1% ± 6.8%	34.6% ± 8.5%	39.0% ± 8.1%†
LHV	19.6% ± 4.9%	19.9% ± 4.4%	19.8% ± 5.5%	18.4% ± 5.9%

Distribution of Branching Patterns				
		Candidate	Donor	*P* Value
Hepatic artery	A1	80.5% (91/113)	82.7% (91/110)	NS
	A2	9.7% (11/113)	7.3% (8/110)	
	A3	9.7% (11/113)	9.0% (10/110)	
Portal vein	PV1	73.4% (83/113)	84.5% (93/110)	NS
	PV2	20.4% (23/113)	11.8% (13/110)	
	PV3	6.2% (7/113)	3.6% (4/110)	

*$P < 0.05$ for I versus II.
†$P < 0.05$ for I versus III.
‡$P < 0.05$ for II versus III.

and portal vein. Because there were no differences in the distribution of the types of hepatic veins or in the development of hepatic veins, the following analyses were performed for all 223 potential donors.

Hepatic Vein

Of the potential donors who were studied, 133 had type I veins (59.6%), 52 had type II veins (23.3%), and 38 had type III veins (17.0%; Fig. 2).

The drainage volume percentages in the whole liver according to the different types of hepatic veins are shown in Table 2. On the basis of the definitions of the hepatic vein types, the percentage of the volume drained by the IRHV increased from type I to type III, whereas the drainage volume of the RHV decreased in that order. In addition, the percentage of the volume that was drained by the LHV did not differ between the different types of veins; however, the volume of the MHV drainage increased similarly to that of the IRHV from type I to type III.

The drainage volume of each hepatic vein in right lobe grafts was compared. When the drainage volume of the IRHV increased in the right lobe, the percentage of the volume that drained from the right lobe by the MHV increased from type I to type III (Table 2). However, in the left lobe, the percentage of the volume drained by the LHV and MHV tributaries did not vary between the 3 types (Table 2). Moreover, with respect to the volume drained from the right lobe by the branches of the MHV [V5 and vein draining segment 8 (V8)], the percentages of both V5 and V8 varied significantly for all 3 types ($P < 0.05$ for V8 and $P < 0.05$ for V5) and increased significantly from type I to type III [for V5, 17.3% ± 8.5% on average, 15.6% ± 7.9% for type I, 18.4% ± 8.4% for type II, and 21.6% ± 9.1% for type III ($P = 0.259$ for I versus II, $P < 0.01$ for I versus III, and $P = 0.050$ for II versus III); for V8, 12.6% ± 5.9% on average, 12.0% ± 5.6% for type I, 12.6% ± 5.0% for type II, and 14.9% ± 7.2% for type III ($P = 0.958$ for I versus II, $P = 0.027$ for I versus III, and $P = 0.108$ for II versus III)].

With type III hepatic veins, the RHV drained 25.1% ± 8.8% of the right lobe, the IRHV drained 30.5% ± 9.3%, and the MHV drained 41.2% ± 11.8%. Each of these 3 veins drained almost one-third of the right lobe, and the MHV provided the greatest drainage.

Portal Vein

The proximal branching patterns of the portal vein were examined with 3D CT (Fig. 1). PV1 was the most frequent pattern (78.9%), and it was followed by PV2 (16.1%) and PV3 (4.9%). The type of hepatic vein was not related to the pattern of proximal portal vein branching. Variations in portal vein branching (group B) were detected in 21.0% of all cases. On the basis of

TABLE 2. Percentage of Drainage in Whole Liver Grafts and in Right and Left Lobe Grafts by Each Hepatic Vein and MHV Tributaries

Graft	Vein	Total (n = 223)	Type I (n = 133)	Type II (n = 52)	Type III (n = 38)
Whole liver (100%)	RHV	35.5% ± 12.2%	42.5% ± 7.5%	31.8% ± 7.8%*	16.2% ± 5.6%†,‡
	IRHV	5.9% ± 7.7%	0.8% ± 1.5%	8.7% ± 3.0%*	19.7% ± 6.2%†,‡
	MHV	33.7% ± 8.1%	32.1% ± 6.7%	33.9% ± 8.3%	39.3% ± 9.5%†,‡
Right lobe (100%)	RHV	55.0% ± 18.1%	65.4% ± 10.3%	50.1% ± 11.0%*	25.1% ± 8.8%†,‡
	IRHV	9.2% ± 11.9%	1.3% ± 2.4%	13.8% ± 4.5%*	30.5% ± 9.3%†,‡
	MHV tributaries	33.5% ± 10.7%	30.9% ± 9.28%	34.5% ± 10.5%*	41.2% ± 11.8%†,‡
Left lobe (100%)	LHV	56.5% ± 13.5%	58.3% ± 11.3%	53.9% ± 14.7%	53.4% ± 17.7%
	MHV tributaries	34.6% ± 10.6%	34.1% ± 9.0%	34.7% ± 10.7%	36.1% ± 14.9%

*$P < 0.05$ for I versus II.
†$P < 0.05$ for I versus III.
‡$P < 0.05$ for II versus III.

TABLE 3. Distribution of the Branching Patterns of the Portal Vein, Hepatic Artery, and Biliary Duct by the Type of Hepatic Vein in Right and Left Lobe Grafts

			Right Lobe		
			Type I	Type II	Type III
Portal vein	Group A	PV1 (n = 176)	79.6% (106/133)	75.0% (39/52)	81.5% (31/38)
	Group B	PV2/PV3 (n = 47)	20.3% (27/133)	25.0% (13/52)	18.4% (7/38)
Hepatic artery	Group A	A1/A3 (n = 202)	93.2% (124/133)	86.5% (45/52)	86.9% (33/38)
	Group B	A2 (n = 21)	6.0% (8/133)	13.5% (7/52)	13.1% (5/38)
Biliary duct	Group A	B1 (n = 55)	55.3% (36/65)	56.0% (14/25)	25.0% (5/20)
	Group B	B2-B5 (n = 55)	44.6% (29/65)	44.0% (11/25)	75.0% (15/20)*,†
			Left Lobe		
			Type I	Type II	Type III
Portal vein	Group A	PV1/PV2 (n = 212)	96.2% (128/133)	94.2% (49/52)	92.2% (35/38)
	Group B	PV3 (n = 11)	3.8% (5/133)	5.8% (3/52)	7.8% (3/38)
Hepatic artery	Group A	A4	56.9% (74/130)	51.9% (27/52)	71.0% (27/38)
	Group B	A5	43.1% (56/130)	48.1% (25/52)	29.0% (11/38)
Biliary duct	Group A	B1-B3 (n = 83)	78.50 (51/65)	80.0% (20/25)	60.0% (12/20)
	Group B	B4/B5 (n = 27)	21.5% (14/65)	20.0% (5/25)	40.0% (8/20)

*$P < 0.05$ for I versus II.
†$P < 0.05$ for I versus III.

the type of hepatic vein, the percentage of portal vein variations was compared. The portal vein branching patterns in both right and left lobes showed no correlation with the patterns of hepatic veins (Table 3).

Hepatic Arteries

A1 was most frequent (81.9%), and it was followed by A2 (9.4%) and A3 (9.0%). The percentages of A4 and A5 were 58.2% and 41.8%, respectively (Fig. 1). The percentage of arterial variations was compared with respect to the type of hepatic vein. The arterial branching patterns in both the right and left lobes showed no significant correlation with the type of hepatic veins; however, in the left lobe graft, A4 tended to be more frequent in the type III hepatic vein ($P = 0.06$).

Biliary Duct

B1 was most frequent (50%), and it was followed by B4 (20%), B2 (15.4%), B3 (10%), and B5 (4.5%; Fig. 1). There was no statistical relationship between the type of hepatic vein and each biliary variation, but B3 was more prevalent with type III veins than type I and type II veins (7.6% for type I, 8% for type II, and 20% for type III; intergroup $P = 0.315$). In right lobe grafts, group B biliary ducts (B2-B5) were detected in 50% of donors. A classification based on the type of hepatic vein indicated that B1 was found in 55.3% (36/65) of patients with type I veins, in 56.0% (14/25) with type

II veins, and in 25.0% (5/20) with type III veins (Table 3). In comparison with patients with type I and II hepatic veins, patients with type III veins had significantly fewer instances of normal branching in the right lobe graft ($P = 0.022$ for type II and $P = 0.041$ for type III). On the other hand, in left lobe grafts, there was no correlation between the type of hepatic vein and the branching patterns of the bile duct.

DISCUSSION

In the current study, we found that the size of the IRHV, which was compared with the RHV, was related to the development of the MHV tributaries in the right lobe. When the IRHV increased, the volume drained by MHV tributaries also increased. In addition, type III hepatic veins, characterized by a large IRHV, were shown to have some characteristics and were found in 17% of potential healthy donors. Type III MHV tributaries provided the largest drainage from the right lobe. Moreover, this type exhibited significantly more biliary duct variation, primarily in the form of an independent posterior branch that originated from the common hepatic duct (B3). On the other hand, we did not find other relationships between the type of hepatic vein and the branching pattern of the portal vein or hepatic artery.

On the basis of autopsies, Nakamura and Tsuzuki[23] revealed relationships between the RHV and the IRHV. They reported that 38.6% of the specimens were hepatic vein type I, 37.3% were type II, and 24.1% were type III; types II and III were more prevalent in their study versus ours. This may have occurred because 16 ± 9 IRHVs on average were counted in their study (even those with the diameter of a pin were included), and only veins with a diameter of 2 mm or larger can be depicted on CT scans.[25] In the current study, the type of hepatic vein was defined by a comparison of the collective volume of the IRHVs with that of the RHV when the CT scan showed multiple IRHVs. However, there were no cases in which the collective volume of multiple small IRHVs accounted for a significant volume in the liver graft. Meanwhile, this 3D CT classification of hepatic veins cannot be used as an indication for IRHV reconstruction. For technical reasons, the diameter of the hepatic vein needs to be sufficiently large for reconstruction (ie, >5 mm).[26]

In comparison with the previous MHV classifications by Marcos et al.[4] and Neumann et al.,[21] the results of the present study permitted an interpretation of the relationship between the IRHV and MHV (Fig. 2). Type I in this study corresponds to an MHV with numerous small tributaries that flow into the main trunk (13%-20%); type II corresponds to an MHV type with symmetrical branching of the veins that drain the superior and inferior parts of segment 4, V5, and V8 (59%-70%); and type III corresponds to a MHV type with large V8 and V5 drainage to segment 6 (10%-18%). As indicated earlier, an increase in the area drained by the MHV from type I to type III was attributable to the fact that the areas draining segments 5 and 8 became larger than those draining segment 4. With type III veins, there was almost no venous flow from the dorsal portion of segments 5 and 8 into the small RHV and IRHV; the drainage of the area occurred via large branches of V8 and V5 flowing into the MHV. With type III veins, V5 accounted for approximately 21% of the drainage of the right lobe. Neumann et al.[21] reported that the volume of drainage differed according to the type of MHV branching and that drainage by V5 in particular differed; this is in agreement with the results of the current study. Therefore, the pattern of MHV branching and the percentage of drainage by the branches can be predicted by the size of the IRHV.

The current study revealed a significantly high prevalence of biliary variations with type III hepatic veins, but the type of hepatic vein did not correlate with the ramification of the portal vein and hepatic artery. Thus, if type III veins are used in a right lobe graft, 75% of patients might require multiple biliary reconstructions. On the other hand, portal vein variations may be related to biliary tree variations. Embryologically, intrahepatic ducts develop from ductal plates after development of the portal duct,[27] and a correlation with portal vein and biliary variations has been reported.[28] Radtke et al.[22] concluded that there is a correlation between a large IRHV and portal vein variations, including proximal and distal variations (we studied only proximal portal vein ramification in this study). Taking these facts into consideration, we should probably keep in mind the extent of the variations of the portal vein and the bile duct when preoperative image evaluations are performed for type III grafts.

In the context of LDLT, for the evaluation of the anatomy of the liver in a patient with a large IRHV before surgery, it is important to (1) confirm the characteristics of MHV branching and the sizes of the branches and (2) detect any possible abnormalities in biliary ramification. Indeed, 20 donors (17%) in our series showed type III hepatic veins. Seven of the 110 recipients (6%) underwent left lobe grafting, whereas 6 patients (5%) received a right lobe graft with a type III hepatic vein because of inadequate left lobe volume for grafting. We performed intraoperative cholangiography for the assessment of biliary anatomy; however, a recent report has suggested that preoperative CT cholangiography is useful for biliary assessment.[29] This study suggests that a preoperative evaluation of the biliary anatomy by CT cholangiography is important when a right lobe graft is being used, especially in the case of a liver with a type III hepatic vein. Meanwhile, the findings of our study suggest that multiple branches of the hepatic artery and bile duct are rarely exposed on the cut surface of the left lobe graft in the case of a type III hepatic vein. Hence, for simple reconstructions, a left lobe graft may be preferable for a liver with a type III hepatic vein if the graft volume is acceptable.

The use of 3D CT for the preoperative evaluation of hepatic vasculatures has become common in LDLT.[30] However, there have been very few reports on the

volumetric and anatomical relationship of hepatic vasculatures of liver grafts. This classification will help us to preoperatively determine the appropriate technique or form of reconstruction.

In conclusion, this study demonstrates the volumetric and anatomical interrelationship of hepatic veins and other hepatic vasculatures for LDLT with 3D CT scanning. According to our findings, a right lobe graft with a large IRHV is accompanied by a large drainage volume via the MHV and by bile duct variations in 17% of livers. Detailed preoperative evaluations are essential for the success of adult LDLT.

REFERENCES

1. Hashikura Y, Makuuchi M, Kawasaki S, Matsunami H, Ikegami T, Nakazawa Y, et al. Successful living-related partial liver transplantation to an adult patient. Lancet 1994;343:1233-1234.
2. Nakamura T, Tanaka K, Kiuchi T, Kasahara M, Oike F, Ueda M, et al. Anatomical variations and surgical strategies in right lobe living donor liver transplantation: lessons from 120 cases. Transplantation 2002;73:1896-1903.
3. Lee S, Park K, Hwang S, Kim K, Ahn C, Moon D, et al. Anterior segment congestion of a right liver lobe graft in living-donor liver transplantation and strategy to prevent congestion. J Hepatobiliary Pancreat Surg 2003;10:16-25.
4. Marcos A, Orloff M, Mieles L, Olzinski AT, Renz JF, Sitzmann JV. Functional venous anatomy for right-lobe grafting and techniques to optimize outflow. Liver Transpl 2001;7:845-852.
5. Hata S, Sugawara Y, Kishi Y, Niiya T, Kaneko J, Sano K, et al. Volume regeneration after right liver donation. Liver Transpl 2004;10:65-70.
6. Yonemura Y, Taketomi A, Soejima Y, Yoshizumi T, Uchiyama H, Gion T, et al. Validity of preoperative volumetric analysis of congestion volume in living donor liver transplantation using three-dimensional computed tomography. Liver Transpl 2005;11:1556-1562.
7. Kasahara M, Takada Y, Fujimoto Y, Ogura Y, Ogawa K, Uryuhara K, et al. Impact of right lobe with middle hepatic vein graft in living-donor liver transplantation. Am J Transplant 2005;5:1339-1346.
8. Campsen J, Hendrickson RJ, Zimmerman MA, Wachs M, Bak T, Russ P, et al. Adult right lobe live donor liver transplantation without reconstruction of the middle hepatic vein: a single-center study of 109 cases. Transplantation 2008;85:775-777.
9. Hwang S, Lee SG, Ahn CS, Kim KH, Moon DB, Ha TY, et al. Technique and outcome of autologous portal Y-graft interposition for anomalous right portal veins in living donor liver transplantation. Liver Transpl 2009;15:427-434.
10. Kasahara M, Egawa H, Tanaka K, Ogawa K, Uryuhara K, Fujimoto Y, et al. Variations in biliary anatomy associated with trifurcated portal vein in right-lobe living-donor liver transplantation. Transplantation 2005;79:626-627.
11. Varotti G, Gondolesi GE, Goldman J, Wayne M, Florman SS, Schwartz ME, et al. Anatomic variations in right liver living donors. J Am Coll Surg 2004;198:577-582.
12. Marcos A, Orloff M, Mieles L, Olzinski A, Sitzmann J. Reconstruction of double hepatic arterial and portal venous branches for right-lobe living donor liver transplantation. Liver Transpl 2001;7:673-679.
13. Kasahara M, Egawa H, Takada Y, Oike F, Sakamoto S, Kiuchi T, et al. Biliary reconstruction in right lobe living-donor liver transplantation: comparison of different techniques in 321 recipients. Ann Surg 2006;243:559-566.
14. Kyoden Y, Tamura S, Sugawara Y, Matsui Y, Togashi J, Kaneko J, et al. Portal vein complications after adult-to-adult living donor liver transplantation. Transpl Int 2008;21:1136-1144.
15. Lerut J, Tzakis AG, Bron K, Gordon RD, Iwatsuki S, Esquivel CO, et al. Complications of venous reconstruction in human orthotopic liver transplantation. Ann Surg 1987;205:404-414.
16. Gondolesi GE, Varotti G, Florman SS, Munoz L, Fishbein TM, Emre SH, et al. Biliary complications in 96 consecutive right lobe living donor transplant recipients. Transplantation 2004;77:1842-1848.
17. Jin MB, Onodera Y, Furukawa H, Todo S. Three-dimensional volumetric analysis for reconstruction of middle hepatic vein tributaries in living donor liver transplantation. J Am Coll Surg 2005;200:468-469.
18. Taniguchi M, Furukawa H, Shimamura T, Suzuki T, Oota M, Onodera Y, et al. Hepatic venous reconstruction of anterior sector using three-dimensional helical computed tomography in living donor liver transplantation. Transplantation 2006;81:797-799.
19. Kamiyama T, Nakagawa T, Nakanishi K, Kamachi H, Onodera Y, Matsushita M, et al. Preoperative evaluation of hepatic vasculature by three-dimensional computed tomography in patients undergoing hepatectomy. World J Surg 2006;30:400-409.
20. Reichert PR, Renz JF, D'Albuquerque LA, Rosenthal P, Lim RC, Roberts JP, et al. Surgical anatomy of the left lateral segment as applied to living-donor and split-liver transplantation: a clinicopathologic study. Ann Surg 2000;232:658-664.
21. Neumann JO, Thorn M, Fischer L, Schobinger M, Heimann T, Radeleff B, et al. Branching patterns and drainage territories of the middle hepatic vein in computer-simulated right living-donor hepatectomies. Am J Transplant 2006;6:1407-1415.
22. Radtke A, Sotiropoulos GC, Molmenti EP, Nadalinl S, Schroeder T, Schenk A, et al. The influence of accessory right inferior hepatic veins on the venous drainage in right graft living donor liver transplantation. Hepatogastroenterology 2006;53:479-483.
23. Nakamura S, Tsuzuki T. Surgical anatomy of the hepatic veins and the inferior vena cava. Surg Gynecol Obstet 1981;152:43-50.
24. Couinaud C. Surgical Anatomy of the Liver Revisited. 2nd ed. Paris, France: Couinaud; 1989.
25. Radtke A, Sgourakis G, Sotiropoulos GC, Molmenti EP, Saner FH, Timm S, et al. Territorial belonging of the middle hepatic vein in living liver donor candidates evaluated by three-dimensional computed tomographic reconstruction and virtual liver resection. Br J Surg 2009;96:206-213.
26. Sugawara Y, Makuuchi M, Sano K, Imamura H, Kaneko J, Ohkubo T, et al. Vein reconstruction in modified right liver graft for living donor liver transplantation. Ann Surg 2003;237:180-185.
27. Desmet VJ. Ludwig symposium on biliary disorders—part I. Pathogenesis of ductal plate abnormalities. Mayo Clin Proc 1998;73:80-89.
28. Lee VS, Morgan GR, Lin JC, Nazzaro CA, Chang JS, Teperman LW, et al. Liver transplant donor candidates: associations between vascular and biliary anatomic variants. Liver Transpl 2004;10:1049-1054.
29. Schroeder T, Malago M, Debatin JF, Goyen M, Nadalin S, Ruehm SG. "All-in-one" imaging protocols for the evaluation of potential living liver donors: comparison of magnetic resonance imaging and multidetector computed tomography. Liver Transpl 2005;11:776-787.
30. Cheng YF, Lee TY, Chen CL, Huang TL, Chen YS, Lui CC. Three-dimensional helical computed tomographic cholangiography: application to living related hepatic transplantation. Clin Transplant 1997;11:209-213.

Another Cause of Autoimmune Hepatitis

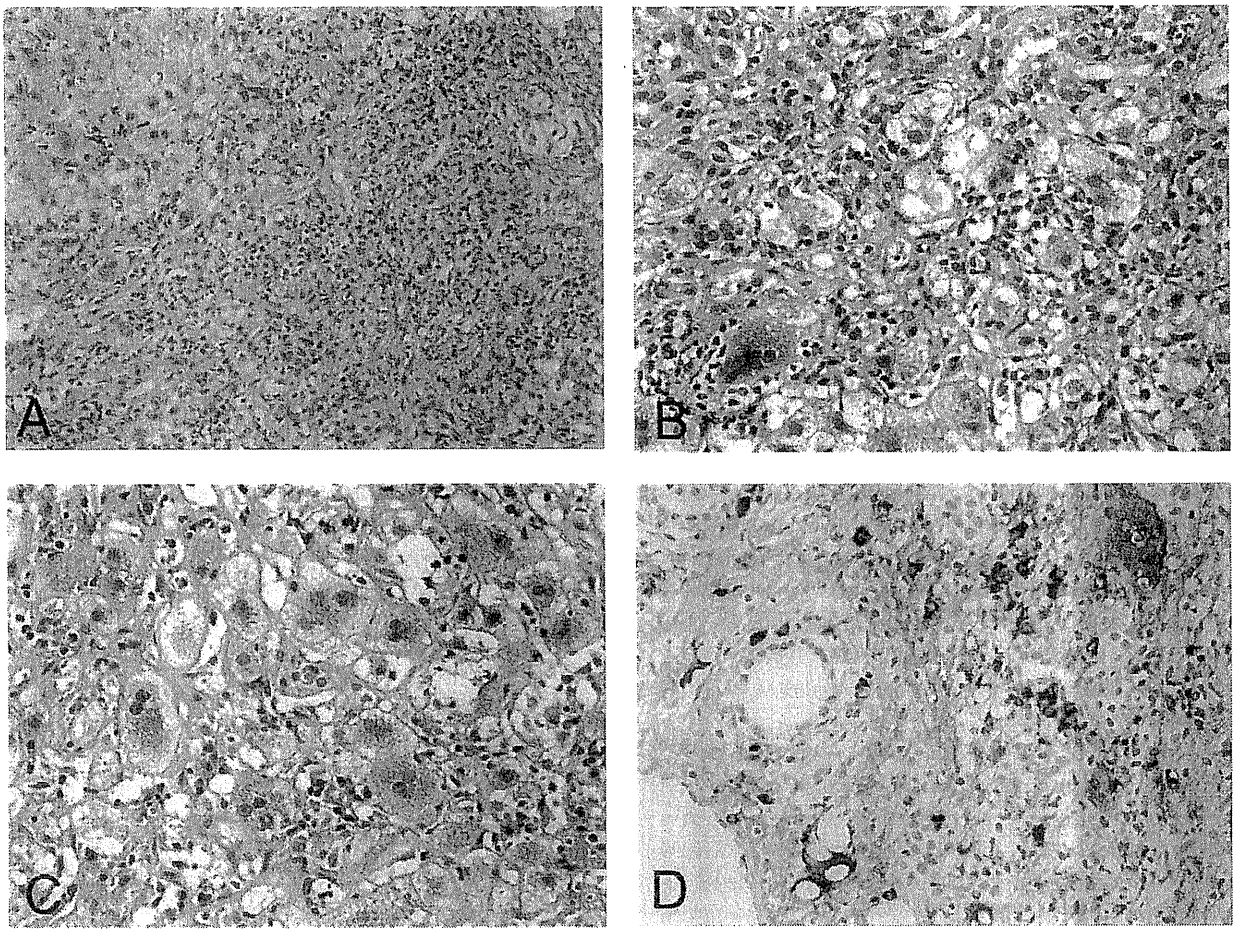

A 42-year-old man was admitted to our hospital because of elevated liver enzymes (aspartate aminotransferase, 642 IU/L [normal range: 12-37]; alanine aminotransferase, 788 IU/L [normal range: 7-45]; alkaline phosphatase, 605 IU/L [normal range: 124-367]; γ-glutamyl transpeptidase, 180 IU/L [normal range: 6-30]; and total bilirubin, 8.6 mg/dL [normal range: 0.3-1.2]). His serum immunoglobulin G (IgG) concentration was 5622 mg/dL (normal range: 870-1700), and anti-nuclear antibody titer (1:20480), anti-double-stranded DNA (>400 IU/mL), and smooth muscle antibody titer (1:40) were all abnormal. Infection with hepatitis A, B, and C; cytomegalovirus; and Epstein-Barr virus were excluded, and no drug use was noted. Ultrasonography, abdominal computed tomography, and magnetic resonance imaging showed no abnormalities of the extrahepatic

Abbreviations: AIH, autoimmune hepatitis; HE, hematoxylin and eosin; IgG, immunoglobulin G.

This study was supported in part by a research grant from the Japanese Ministry of Health, Labour, and Welfare and a Shinshu University Grant-in-Aid for Young Scientists of Exploratory Research.

Address reprint requests to: Takeji Umemura, M.D., Ph.D., Department of Internal Medicine, Shinshu University School of Medicine, 3-1-1 Asahi, Matsumoto 390-8621, Japan. E-mail: tumemura@shinshu-u.ac.jp; fax: +81-263-32-9412.

Published online in Wiley InterScience (www.interscience.wiley.com).

DOI 10.1002/hep.23730

Potential conflict of interest: Nothing to report.

bile ducts or pancreas. The first liver biopsy showed changes associated with typical autoimmune hepatitis (AIH); liver parenchyma was collapsed with broad fibrous septa containing entrapped hepatocytes, and lymphoplasmacytic infiltration with interface activity was seen (Fig. 1A; hematoxylin and eosin [H&E] staining, magnification ×200). Hepatocytes showed rosetting in numerous places (Fig. 1B; H&E staining, magnification ×400). Lobular inflammation was evident with giant cell change of hepatocytes (Fig. 1C; H&E staining, magnification ×400), but no biliary epithelial changes were found. The patient fulfilled the criteria for definite AIH by the International Autoimmune Hepatitis Group and was administered corticosteroids at 60 mg/day, which led to improvement of laboratory findings. Prior to treatment, however, the patient's serum IgG4 concentration was 642 mg/dL (normal: ≤ 135) in a stored serum sample, and immunostaining of liver tissue showed abundant plasma cells with strong immunohistochemical reactivity to IgG4 in a portal tract (Fig. 1D; IgG4 immunostaining, magnification ×400). A second liver biopsy performed 7 months afterward showed remaining portal sclerosis, but lobular distortion and portal inflammation were ameliorated, and serum alanine aminotransferase and IgG4 concentrations were normalized. IgG4-positive plasma cells were scarce in portal tracts (data not shown).

In an earlier report, a strong and unexpected association was seen between serum IgG4 concentration and IgG4-bearing plasma cell infiltration in the liver of a case with type 1 AIH, raising the possibility of a new disease entity termed IgG4-associated AIH.[1] Raised serum IgG4 concentration and IgG4-bearing plasma cell infiltration have a high sensitivity and specificity for the diagnosis of IgG4-related diseases.[2-4] Similar to the present case, histological findings in the liver of patients with IgG4-associated AIH showed bridging fibrosis, portal inflammation with abundant plasma cell infiltration, interface hepatitis, and lobular hepatitis. More interestingly, giant cell change and rosette formation were obvious as well. These two cases imply that IgG4-related inflammatory processes can occur in the hepatic parenchyma similarly to those in the pancreatobiliary system, and such cases may resemble AIH both clinically and pathologically. On the contrary, Chung et al. described IgG4-associated AIH as patients with AIH who had IgG4-positive plasma cells in the liver.[5] Because no cases showed high serum IgG4 in their cohort, we believe they are different from our two representative patients and thus should not be classified as an IgG4-related disease. Koyabu et al. recently reported that an IgG4/IgG1-bearing plasma cell ratio of >1 in the liver is specific for IgG4-related diseases.[6] In our patient, the IgG4/IgG1 ratio was >1 (data not shown) and consistent with their findings, which provides further evidence of our case as an IgG4-related disorder. Because IgG4-associated AIH is clearly an IgG4 hepatopathy, this disease should be differentiated from classical AIH. Detection of IgG4 and assessment of liver histology using IgG4 immunostaining may be useful for distinguishing IgG4-related diseases from classical AIH.

TAKEJI UMEMURA, M.D., PH.D.[1]
YOH ZEN, M.D., PH.D.[2,3]
YASUNI NAKANUMA, M.D., PH.D.[3]
KENDO KIYOSAWA, M.D., PH.D.[1]
[1]*Department of Internal Medicine, Division of Hepatology and Gastroenterology, Shinshu University School of Medicine, Matsumoto, Japan*
[2]*Division of Pathology, Kanazawa University Hospital, Kanazawa, Japan*
[3]*Department of Human Pathology, Kanazawa University Graduate School of Medicine, Kanazawa, Japan*

References

1. Umemura T, Zen Y, Hamano H, Ichijo T, Kawa S, Nakanuma Y, et al. IgG4 associated autoimmune hepatitis: a differential diagnosis for classical autoimmune hepatitis. Gut 2007;56:1471-1472.
2. Hamano H, Kawa S, Horiuchi A, Unno H, Furuya N, Akamatsu T, et al. High serum IgG4 concentrations in patients with sclerosing pancreatitis. N Engl J Med 2001;344:732-738.
3. Zen Y, Harada K, Sasaki M, Sato Y, Tsuneyama K, Haratake J, et al. IgG4-related sclerosing cholangitis with and without hepatic inflammatory pseudotumor, and sclerosing pancreatitis-associated sclerosing cholangitis: do they belong to a spectrum of sclerosing pancreatitis? Am J Surg Pathol 2004;28:1193-1203.
4. Umemura T, Zen Y, Hamano H, Kawa S, Nakanuma Y, Kiyosawa K. Immunoglobin G4-hepatopathy: association of immunoglobin G4-bearing plasma cells in liver with autoimmune pancreatitis. HEPATOLOGY 2007;46:463-471.
5. Chung H, Watanabe T, Kudo M, Maenishi O, Wakatsuki Y, Chiba T. Identification and characterization of IgG4-associated autoimmune hepatitis. Liver Int 2010;30:222-231.
6. Koyabu M, Uchida K, Miyoshi H, Sakaguchi Y, Fukui T, Ikeda H, et al. Analysis of regulatory T cells and IgG4-positive plasma cells among patients of IgG4-related sclerosing cholangitis and autoimmune liver diseases. J Gastroenterol 2010; doi:10.1007/s00535- 010-0199-3.

Research Article

EASL EUROPEAN ASSOCIATION FOR THE STUDY OF THE LIVER | JOURNAL OF HEPATOLOGY

Association analysis of *cytotoxic T-lymphocyte antigen 4* gene polymorphisms with primary biliary cirrhosis in Japanese patients

Satoru Joshita[1], Takeji Umemura[1,*], Kaname Yoshizawa[1], Yoshihiko Katsuyama[2], Eiji Tanaka[1], Minoru Nakamura[3], Hiromi Ishibashi[3], Masao Ota[4], The Shinshu PBC Study Group[†]

[1]*Department of Medicine, Division of Gastroenterology and Hepatology, Shinshu University School of Medicine, 3-1-1 Asahi, Matsumoto 390-8621, Japan;* [2]*Department of Pharmacy, Shinshu University Hospital, 3-1-1 Asahi, Matsumoto 390-8621, Japan;* [3]*Clinical Research Center, National Hospital Organization (NHO), Nagasaki Medical Center and Department of Hepatology, Nagasaki University Graduate School of Biomedical Sciences, 2-1001-1 Kubara, Omura 856-8562, Japan;* [4]*Department of Legal Medicine, Shinshu University School of Medicine, 3-1-1 Asahi, Matsumoto 390-8621, Japan*

Background & Aims: Primary biliary cirrhosis (PBC) is an organ-specific autoimmune disease of still unidentified genetic etiology that is characterized by chronic inflammation of the liver. Since *cytotoxic T-lymphocyte antigen 4* (*CTLA4*) polymorphisms have recently been linked with PBC susceptibility in studies on Caucasians, we investigated the genetic association between *CTLA4* polymorphisms and PBC in a Japanese population.

Methods: Five single nucleotide polymorphisms (SNPs) in the *CTLA4* gene (rs733618, rs5742909, rs231775, rs3087243, and rs231725) were genotyped in 308 patients with PBC and 268 healthy controls using a TaqMan assay.

Results: One *CTLA4* gene SNP (rs231725) was significantly associated with susceptibility to anti-mitochondrial antibody (AMA)-positive PBC, but clinical significance disappeared after correction for multiple testing. Moreover, *CTLA4* gene SNPs did not influence AMA development or disease progression to orthotopic liver transplantation in our Japanese cohort. In haplotype analyses, one haplotype [haplotype 1 (CGGA)] at rs5742909, rs231775, rs3087243, and rs231725, was significantly associated with susceptibility to both AMA-positive PBC and overall PBC.

Conclusions: This study showed that *CTLA4* gene polymorphisms had a modest, but significant association with susceptibility to PBC in the Japanese population. The connection between genetic variants and the function of the *CTLA4* gene remains to be addressed in future investigations.

Keywords: Primary biliary cirrhosis; Single nucleotide polymorphisms; Cytotoxic T-lymphocyte antigen 4; Genetic susceptibility.

Received 2 October 2009; received in revised form 29 March 2010; accepted 31 March 2010; available online 25 May 2010

* Corresponding author. Tel.: +81 263 37 2634; fax: +81 263 32 9412.

E-mail address: tumemura@shinshu-u.ac.jp (T. Umemura).

† The Shinshu PBC Study Group: Michiharu Komatsu, Naoki Tanaka, Tetsuya Ichijo, Akihiro Matsumoto.

Abbreviations: PBC, primary biliary cirrhosis; AMA, anti-mitochondrial antibody; CTLA4, cytotoxic T-lymphocyte antigen 4; OLT, orthotopic liver transplantation; SNPs, single nucleotide polymorphisms; UTR, untranslated region; LD, linkage disequilibrium; HWE, Hardy–Weinberg equilibrium; *pc*, corrected *p*; OR, odds ratio; CI, confidence interval; sCTLA4, soluble isoform of CTLA4.

Introduction

Primary biliary cirrhosis (PBC) is a liver-specific autoimmune disease characterized by female preponderance and the destruction of intrahepatic bile ducts that often results in cirrhosis and hepatic failure [1]. The etiology of PBC has yet to be conclusively elucidated, although genetic factors are considered to play a prominent role in family and population studies [2–5]. Prior reports have shown the HLA-*DRB1*08* allele to be a weak and regional determinant of PBC susceptibility [6–8]. However, HLA alone does not explain the entire genetic predisposition to PBC, mainly because at least 80–90% of patients with the disease do not carry the most common HLA susceptibility alleles. In this regard, other non-HLA genes are thus being considered to contribute to disease development [9,10].

PBC displays immunologically characteristic features like biliary lymphocytic infiltrates, anti-mitochondrial antibodies (AMA) against the inner lipoyl domain of the E2 subunits of the pyruvate dehydrogenase complex, and elevated serum levels of IFN-γ and TNF-α. The serologic hallmark of PBC is the presence of AMA [11,12], which are found in 95% of patients with PBC [13] and have a specificity of 98% for the disease [12]. Auto-reactive $CD4^+$ and $CD8^+$ T cells are also found in high concentrations in the portal triads of patients with PBC, often surrounding and infiltrating necrotic bile ducts [14–16]. A recent study suggested that a reduction in the number of $CD4^+CD25^+$ regulatory T cells in livers affected with PBC contributed to disease progression [17]. Accumulating data such as these, support a direct role of T-lymphocytes in the pathogenesis of PBC.

The cytotoxic T-lymphocyte antigen 4 (CTLA4) is an inhibitory receptor expressed on the cell surface of activated memory T cells and $CD4^+CD25^+$ regulatory T cells that acts largely as a negative regulator of T-cell responses. Since the potential inhibitory functions of CTLA4 [18] may also trigger a breakdown of immunological self-tolerance, polymorphisms affecting these processes could have significant effects on susceptibility to autoimmunity.

The *CTLA4* gene is a primary candidate for genetic susceptibility to autoimmune diseases, including type 1 diabetes, auto-

immune hepatitis [19,20], and autoimmune pancreatitis [21]. In particular, two single nucleotide polymorphisms (SNPs), rs231775 (49AG) and rs3087243 (CT60), have been widely studied in PBC [22–24]. Although early studies found an association between SNP 49G coding and PBC [22–24], ensuing reports showed negative relationships with susceptibility [25–30] or a positive association with liver damage [31]. A recent investigation reported that rs231725 in the 3′ flanking region of *CTLA4* is associated with AMA-positive PBC in Caucasians [27]. In addition to *CTLA4* polymorphisms, HLA class II, IL12A, IL12RB, and several other candidate SNPs were disclosed as predisposition genes for PBC by a high-density genome-wide association study [9]. Since these SNPs have not been extensively examined in a large Japanese population, the present study sought to evaluate the involvement of *CTLA4* SNPs and haplotype SNPs in susceptibility to PBC and disease progression in Japanese patients.

Patients and methods

Subjects

We analyzed a total of 576 subjects (308 PBC patients and 268 healthy controls) collected from two different regions of Japan (Table 1). Cohort 1 consisted of 198 patients clinically diagnosed with PBC (173 women, median age 58 years old) and 170 healthy subjects who were seen at Shinshu University Hospital, Matsumoto, Japan. Cohort 2 consisted of 110 patients clinically diagnosed with PBC (92 women, median age 61 years old) and 98 healthy subjects from the National Hospital Organization Nagasaki Medical Center, Omura, Japan. The racial background of all subjects was Japanese. Control subjects were volunteers from hospital staff who had indicated the absence of any major illnesses in a standard questionnaire. The diagnosis of PBC was based on criteria from the American Association for the Study of Liver Diseases [32]. Serum AMA, specific for the pyruvate dehydrogenase complex-E2 component, was measured by the enzyme-linked immunosorbent assay as reported previously [33]. An index of greater than seven was considered a positive result. All patients were negative for hepatitis B surface antigen, antibody to hepatitis C virus, and antibody to human immunodeficiency virus. To evaluate associations between SNPs and disease progression, patients were classified into two stages based on their most recent follow-up [34]: early stage patients were histologically in Scheuer stage I or II [35,36] or of unknown histological stage without liver cirrhosis, and late stage patients were histologically in Scheuer stage III or IV or clinically diagnosed with liver cirrhosis or hepatic failure. All participants provided informed written consent for this study, which had been approved by the institutional ethics committee.

CTLA4 SNP genotyping

Genomic DNA from patients and controls was isolated by phenolic extraction of sodium dodecyl sulfate-lysed and proteinase K-treated cells, as described previously [37,38], and adjusted to 10–15 ng/μl.

The five *CTLA4* gene SNPs examined in this study (rs733618, rs5742909, rs231775, rs3087243, and rs231725) were genotyped using the 5′ nuclease (TaqMan) assay using primer, probes, and reaction conditions as recommended by the manufacturer (Applied Biosystems, Tokyo, Japan). These SNPs were selected based on previous reports [21–23,26,27], and were all located in the *CTLA4* gene; SNPs rs733618 and rs5742909 were in the promoter region, SNP rs231775 in exon 1, and SNPs rs3087243 and rs231725 in the 3′ untranslated region (UTR). Polymerase chain reaction was performed with a TaqMan Assay for Real-Time PCR (7500 Real-Time PCR System; Applied Biosystems) following the manufacturer's instructions.

Haplotype–genotype estimation

The R package "haploview" [39] was used to evaluate the haplotype structure of the five examined *CTLA4* SNPs. Pairwise linkage disequilibrium (LD) patterns and haplotype frequency analysis for all SNPs in patients and controls were assessed by the block definition by Gabriel et al. [40].

Table 1. Demographic and clinical data of patients with PBC at study onset.

Characteristics	Cohort 1 Shinshu $n = 198$	Cohort 2 Nagasaki $n = 110$	Combined $n = 308$
Age, years[a]	58 (30–83)	61 (34–85)	58 (30–88)
Female/Male	173/25	92/18	265/43
Disease progression			
Early stage, *n*/Late stage, *n*	149/49	74/36	223/85
Orthotopic liver transplantation, *n* (%)	15 (7.6)	2 (1.8)	17 (5.5)
AMA positive, *n* (%)	171 (86.4)	102 (92.8)	273 (88.6)

PBC, primary biliary cirrhosis; AMA, anti-mitochondrial antibody specific for the pyruvate dehydrogenase complex-E2 component.
[a] Median (range).

Statistical analysis

The Hardy–Weinberg equilibrium (HWE) test was done for each SNP between control and patient groups. The significance of allele distribution between PBC patients and healthy controls was assessed using the χ^2-test with the use 2 × 2 or 2 × 3 comparisons. Fisher's exact probability test was used for groups with fewer than 5 samples. A p value of less than 0.05 was considered statistically significant; p values were corrected using Bonferroni's correction by multiplying by the number of different alleles observed in each locus (pc).

Results

In total, five SNPs located in the *CTLA4* gene were genotyped in 198 patients with PBC and 170 healthy controls in cohort 1 and 110 patients with PBC and 98 healthy controls in cohort 2 (Table 2). Hardy–Weinberg equilibrium (HWE) was observed for all 5 of the examined SNPs in both control groups, and the minor allele frequencies of all SNPs were greater than 5%. In cohort 1, one SNP (rs733618) differed significantly from HWE ($p = 0.03$) (Table 2), and the frequency of the minor A allele at rs231775 was significantly decreased (33.9% vs. 41.5%, odds ratio (OR) 0.72, 95% confidence interval (95% CI) 0.53–0.99, $p = 0.042$, $pc = 0.209$) in 171 AMA-positive PBC patients compared with controls. Positivity for the major G allele (A/G + G/G) at rs231775 was significantly higher in patients with AMA-positive PBC than in healthy subjects (88.3% vs. 79.1%, OR 1.96, 95% CI 1.08–3.53, $p = 0.026$, $pc = 0.128$). Additionally, the allele frequency (61.7% vs. 53.2%, OR 1.41, 95% CI 1.04–1.92, $p = 0.025$, $pc = 0.127$) and allele carrier frequency (86.0% vs. 75.9%, OR 1.96, 95% CI 1.12–3.41, $p = 0.018$, $pc = 0.089$) of the major A allele at rs231725 were significantly increased in AMA-positive PBC patients compared with healthy controls. However, these statistical significances disappeared after correction for multiple testing. No significant differences were observed among the 5 SNPs in cohort 2. The allele frequency (60.3% vs. 53.4%, OR 1.33, 95% CI 1.04–1.69, $p = 0.022$) of the major A allele at rs231725 was significantly increased in combined analysis (cohorts 1 and 2) of 273 AMA-positive PBC patients compared with 268 healthy controls (Table 3), but statistical significance was lost after correction for multiple testing ($pc = 0.110$) (Table 3).

Pairwise LD mapping confirmed that all alleles were in strong LD with an index of >0.8. A strong LD was detected in the same block for PBC patients and controls. We next evaluated haplotype association among AMA-positive PBC patients and healthy subjects in a combined analysis. To estimate haplotype frequencies and analyze haplotype association with PBC, we selected tag SNPs